Published OnlineFirst April 10, 2018; DOI: 10.1158/1535-7163.MCT-17-0937

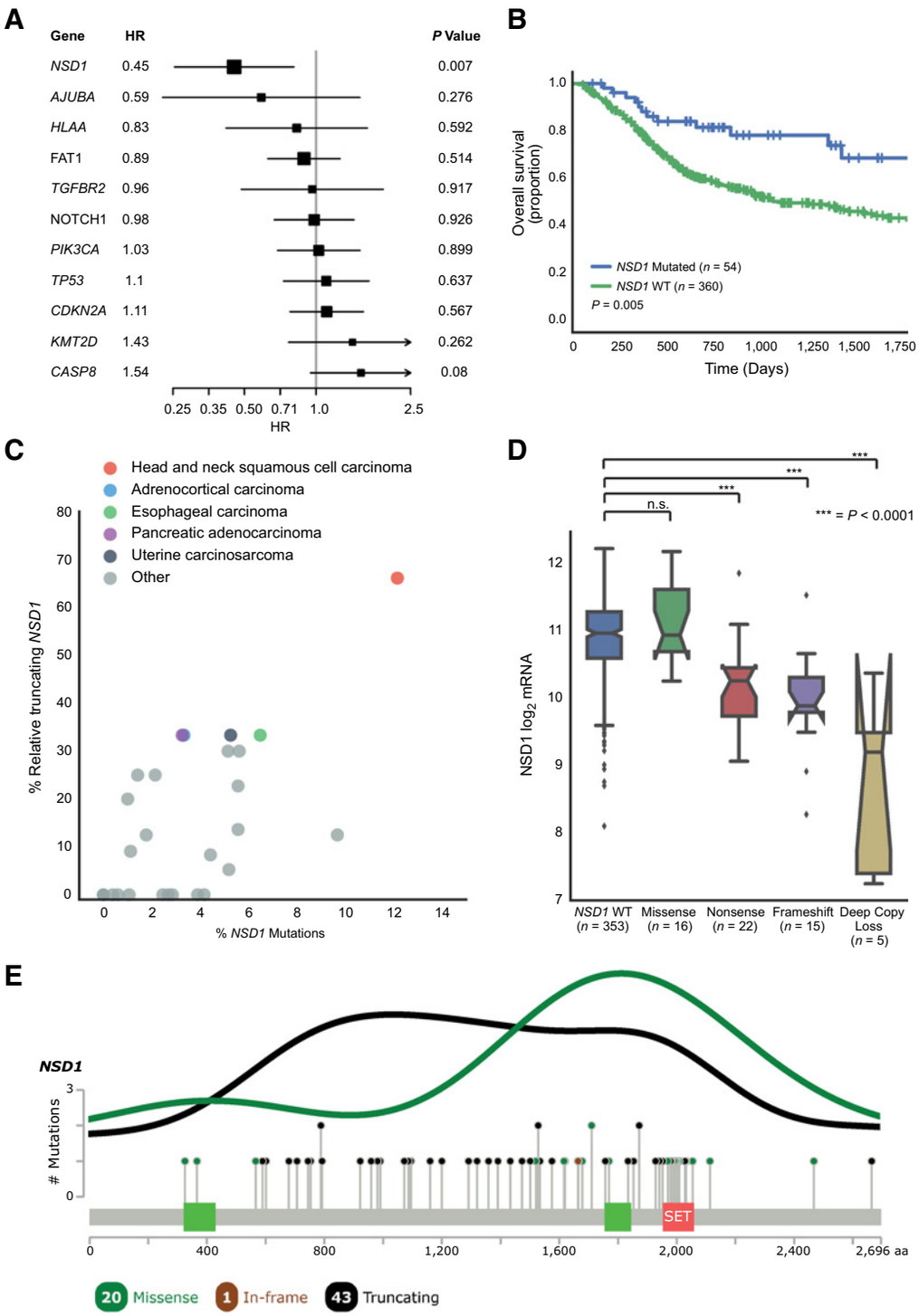

Figure 1.

NSD1 mutations are associated with improved survival in the HPV(−) HNSCC cohort in TCGA. **A,** Forest plot of the prognostic influence of the 11 most recurrently mutated genes in the HPV(−) HNSCC cohort in TCGA. Hazard ratios derived from Cox proportional hazards model incorporating the clinical covariates age, stage, grade, gender, smoking status, and anatomical location. **B,** Kaplan–Meier curve showing overall survival from the HPV(−) HNSCC cohort in TCGA. **C,** Head and neck cancer possess a high percentage of *NSD1* mutations and a high percentage of relative truncating mutations. **D,** Loss-of-function *NSD1* mutations and homozygous deletions, defined as a −2 copy number change by GISTIC (45), have significantly lower gene expression than wild-type or missense mutations. **E,** Lollipop plot of location of *NSD1* mutations as generated by cBioPortal (46, 47). The lines represent density plots of truncating (black) and missense (green) mutations.

Published OnlineFirst April 10, 2018; DOI: 10.1158/1535-7163.MCT-17-0937

Patients with mutations in *NSD1* had a markedly improved clinical outcome, with an approximately 5-year absolute increase in median overall survival time (8.0 vs. 3.1 years; Fig. 1B). Interestingly, patients with *NSD1* mutations were enriched for those with a history of smoking ($P = 0.002$, χ^2 test). When restricting analysis to only current and former smokers, those with *NSD1* mutations had significantly improved survival relative to wild type (HR 0.46, $P = 0.008$, Cox Proportional Hazards; Supplementary Fig. S1A–S1B). There were too few *NSD1* mutations in non-smokers to evaluate the corresponding survival effects for those patients. This survival advantage was validated in a second, independent cohort of 68 HPV(–) HNSCC patients from the University of Chicago (21). In this second cohort, *NSD1*-mutated patients demonstrated an improvement in both progression-free and overall survival (Supplementary Fig. S1C–S1D).

When *NSD1* was examined across other tissue cohorts in TCGA, we found that HNSCC was the tissue with both the highest percentage of *NSD1* mutations (12.2% of patients) and the highest percentage of deleterious mutations (66% of *NSD1* mutations), reflecting a tissue-specific phenotype (Fig. 1C). In the HPV(–) HNSCC cohort, loss-of-function *NSD1* alterations (i.e., nonsense mutations, frameshift mutations or homozygous copy number deletions) were associated with significantly lower mRNA expression levels (Fig. 1D). Missense mutations did not significantly impact *NSD1* mRNA expression levels but tended to cluster near the SET domain (Fig. 1E). To investigate the pathogenicity of these missense mutations, we separated tumors with truncating loss-of-function *NSD1* alterations into a distinct group from those with missense *NSD1* mutations and tested the association of each group with survival. Strikingly, patients with *NSD1* missense mutations had increased survival compared to *NSD1* wild-type patients ($P = 0.042$ by Log-Rank Test, Supplementary Fig. S1E), with an effect that was indistinguishable from *NSD1* loss-of-function mutations. This evidence suggested that the SET domain in *NSD1* is important to the function of the protein, such that missense mutations in this domain lead to loss-of-function of *NSD1*.

NSD1 is a key regulator of the epigenome

Given the role of *NSD1* as an HMT, we sought to determine whether somatic mutations in *NSD1* in HPV(–) head and neck cancer patients might also be associated with CpG hypomethylation. Therefore, we hierarchically clustered the HPV(–) HNSCC samples from TCGA for which CpG methylation data were available ($n = 421$) based on the methylation status of 500 selected CpG sites (Materials and Methods). We found that most patients with mutations in *NSD1* were placed in the same cluster due to a clear pattern of hypomethylated CpG sites (Fig. 2A). Loss-of-function alterations comprised the majority of this cluster whereas missense mutations were more likely to be outliers.

To determine whether disruptions in other genes also correlated with changes in CpG methylation, we examined every gene that was mutated in more than 5% of the HPV(–) HNSCC samples in TCGA ($n = 132$) and determined the percentage of CpG sites that were differentially methylated between wild-type and mutant tumors. Whereas about 14% of CpG sites were differentially mutated between *NSD1* mutant and wild-type tumors, no other gene mutation impacted more than 2% of CpG sites (Fig. 2B). For the *NSD1*-associated differentially methylated CpG sites, a

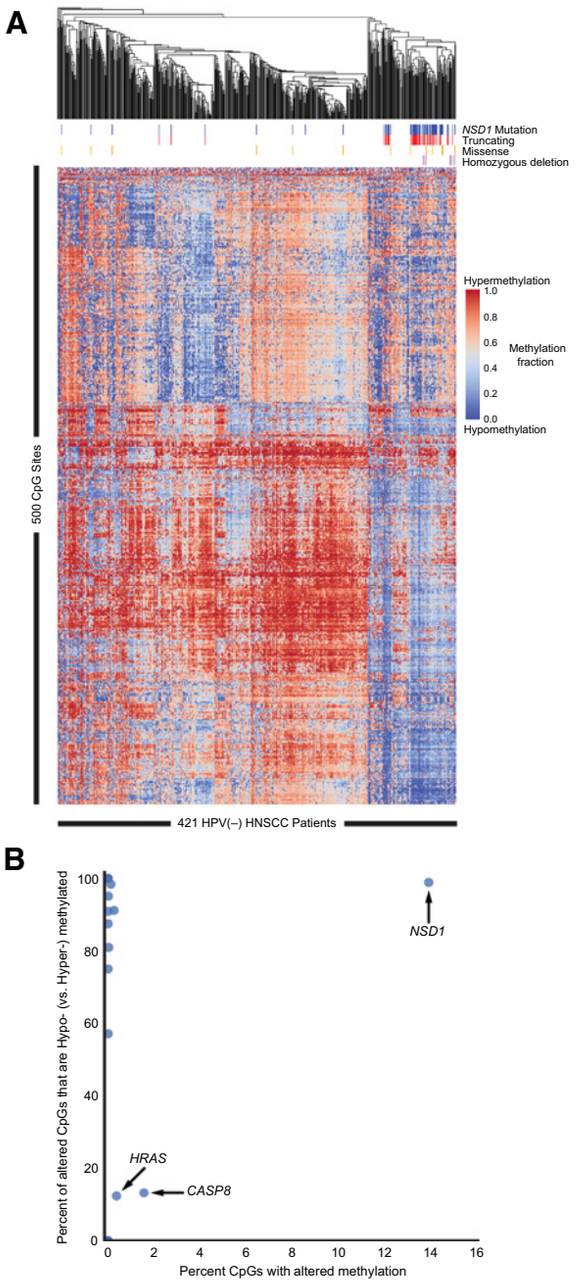

Figure 2.

CpG hypomethylation in patients with *NSD1* loss-of-function mutations in the HPV(–) HNSCC cohort in TCGA. **A,** Unsupervised hierarchical clustering based on the methylation status of 500 selected CpG sites reveals a tight cluster of hypomethylation centered around *NSD1* mutations (blue ticks). Analysis of *NSD1* alteration type reveals that missense mutations (orange ticks) were more likely to be outliers, whereas truncating (red ticks) and homozygous deletions (purple ticks) were associated with the hypomethylation signal. **B,** Gene level methylation analysis reveals that *NSD1* is the only gene where mutations cause a significant change to the methylome (*x*-axis: ∼13% of all CpG sites) with all other genes at <2%. The direction of methylation changes is strikingly in the hypomethylated direction with 98.9% of differentially methylated CpG probes being hypomethylated (*y*-axis).

Published OnlineFirst April 10, 2018; DOI: 10.1158/1535-7163.MCT-17-0937

striking 98.9% were hypomethylated. Therefore, the profound association between genetic alteration and hypomethylation is unique to *NSD1*.

Next, we asked whether CpG hypomethylation in tumors with *NSD1* mutations is preferentially located in any particular region of the genome. Using a sliding window consisting of 200 consecutive CpG sites along each chromosome, we identified a region enriched for hypomethylated CpGs on chromosome 6 (Supplementary Fig. S2). This hypomethylated region includes the MHC I and MHC III loci as well as genes that regulate connective tissue and skin structure (Supplementary Table S1).

Disrupting *NSD1* in HNSCC cell lines leads to CpG hypomethylation

To determine whether disruptions to *NSD1* are sufficient to alter CpG methylation levels, and the dependence of this effect on HPV status, we used CRISPR-Cas9 to generate three monoclonal cell lines with NSD1 truncating mutations. In each case, at least one allele of *NSD1* was disrupted by CRISPR, leading to decreased protein expression levels (Supplementary Fig. S3A–S3D). Methylation status in the parental or *NSD1* disrupted cell lines was determined using the Illumina MethylationEpic BeadChip, which measures CpG methylation levels at >850,000 CpG sites. For each pair of parental and *NSD1* disrupted cell lines, we examined the methylation levels for the 10,000 most differentially methylated CpG sites (Materials and Methods). Substantial hypomethylation was also observed in all *NSD1* disrupted cell lines, regardless of HPV status (Fig. 3A–D). The associated differentially methylated regions (DMRs) were consistently enriched in enhancer and intergenic regions, and depleted in promoter regions. This finding is consistent with observations in TCGA patients with *NSD1* mutations and patients with Sotos Syndrome (22), a childhood disease caused by germline mutations in *NSD1* (Supplementary Fig. S4A).

Analysis of the hypomethylated CpG sites revealed eight genes with differentially hypomethylated CpGs in all three *NSD1* disrupted cell lines and across HNSCC tumors (Supplementary Table S2). The expression levels of some of these genes have been associated with chemotherapy response or implicated as tumor suppressors (Supplementary Table S2). We found that four of these genes were expressed at detectable levels in HNSCC TCGA patients, of which three were significantly downregulated when *NSD1* was mutated (Student *t* Test): *COL13A1* ($P = 4.1 \times 10^{-3}$), *NTM* ($P = 1.3 \times 10^{-2}$), and *PDE1A* ($P = 4.7 \times 10^{-2}$). We performed RT-qPCR on these three genes to determine whether disrupting *NSD1* leads to similar expression changes as observed in patients. Indeed, two of these genes were consistently downregulated by *NSD1* disruption in two distinct cell lines (Supplementary Fig. S4B–S4C).

NSD1 disruption confers sensitivity to cisplatin

Given reported associations between DNA hypomethylating agents and platinum sensitivity (23–26), we hypothesized that the improved survival of *NSD1*-mutated patients might be due to increased sensitivity to cisplatin, a common chemotherapy used to treat HNSCC patients. In each case, cell lines with *NSD1* disruption were more sensitive to cisplatin than the parental wild-type cell lines (Fig. 4A–C). To mimic the loss of *NSD1* pharmacologically, we performed a separate experiment in

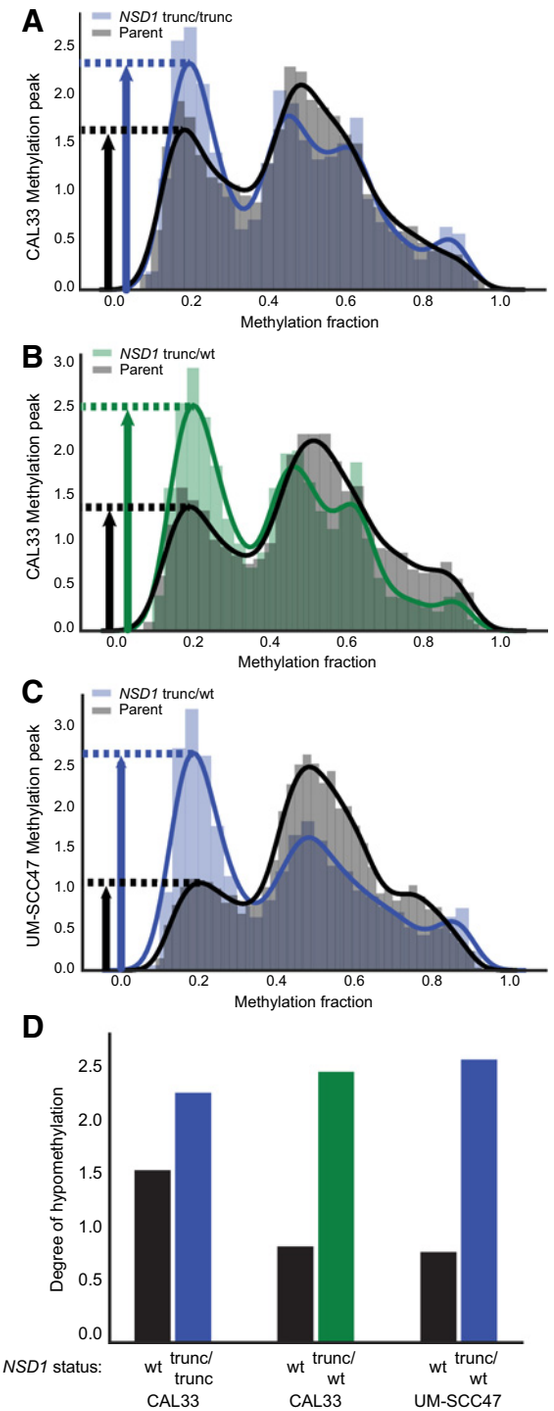

Figure 3.

CpG hypomethylation in cell lines with *NSD1* disrupted. **A** and **B,** Methylation analysis of top 10,000 most differentially methylated CpG sites in CAL33 with and without *NSD1* disrupted demonstrates that the cell lines with *NSD1* disrupted have a much higher hypomethylation peak than their respective parents. **C,** Same as A and B except for UM-SCC47. **D,** Bar plot of the above three cell lines showing the increase in the hypomethylation peak in the *NSD1* disrupted cell lines. *NSD1* alleles from monoclonal populations are characterized as follows: wt, wild type; trunc, contains a truncating mutation.

Published OnlineFirst April 10, 2018; DOI: 10.1158/1535-7163.MCT-17-0937

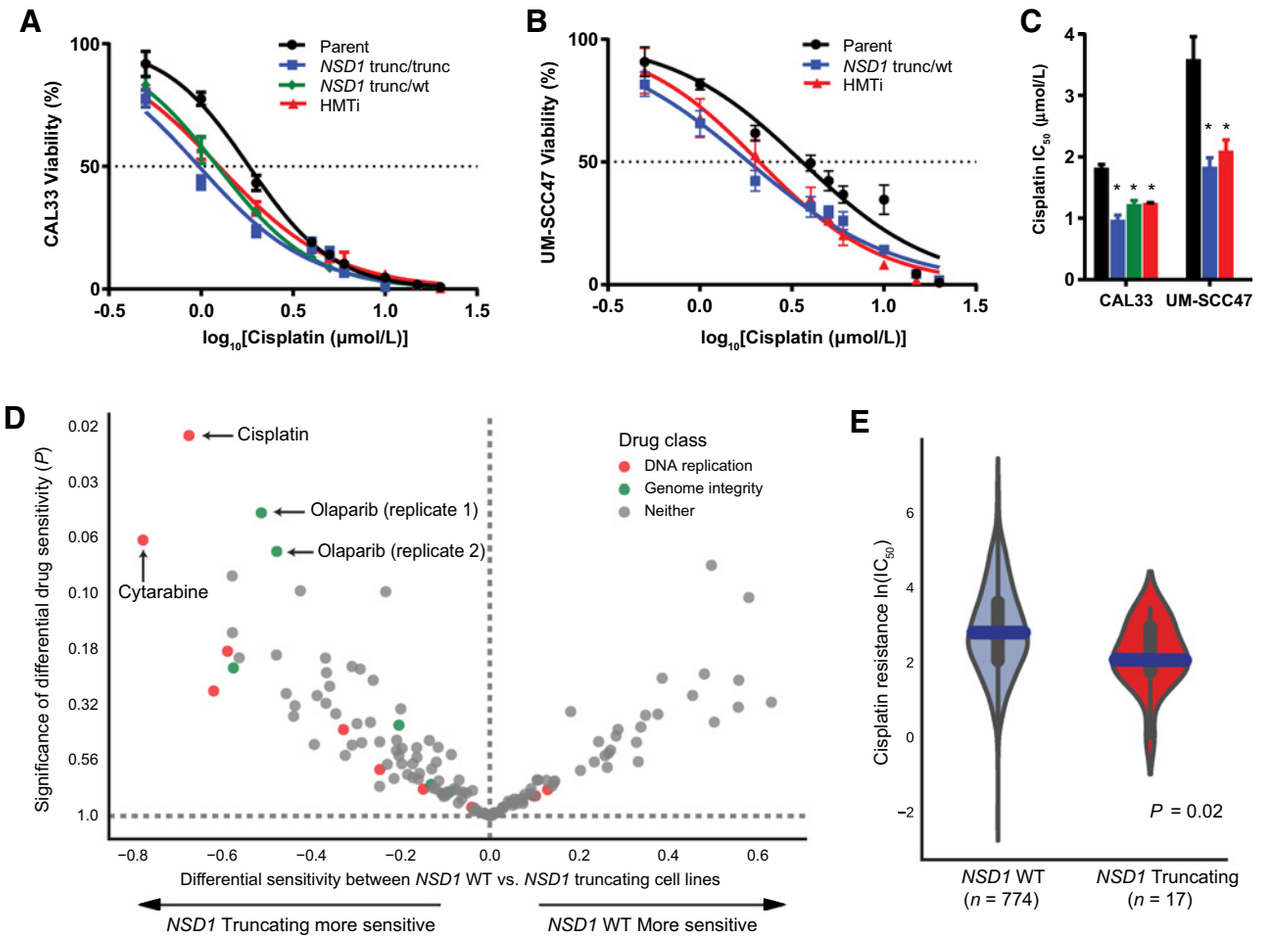

Figure 4.

NSD1 loss-of-function mutations confer increased cisplatin sensitivity. **A** and **B,** Cisplatin sensitivity curves for cell lines with and without *NSD1* disruption, showing greater sensitivity in the disrupted cell lines (blue and green lines). Pretreatment with the HMT inhibitor UNC0379 (HMTi) also increased sensitivity to cisplatin. *NSD1* alleles from monoclonal populations are characterized as follows: wt, wild type; trunc, contains a truncating mutation. **C,** Barplot of cisplatin IC_{50} in parental cell lines and cell lines with *NSD1* disrupted. Asterisk (*) indicates f sum-of-squares $P < 0.0001$ when compared to parental cell line. **D,** Volcano plot showing differential effect of 143 drugs on *NSD1* mutated versus *NSD1* wild-type cell lines. Cisplatin is highly effective (2nd most left point) and the most significant (most upward point). The drug classes "DNA replication" and "Genome integrity" are highly represented on the *NSD1* sensitizing side. **E,** Violin plot showing increased sensitivity of *NSD1*-mutated cell lines to cisplatin.

which parental cells were pre-treated with the HMT inhibitor UNC0379, which also rendered the HNSCC cell lines more sensitive to cisplatin with a growth response that was nearly identical to direct *NSD1* disruption (Fig. 4A–B). To investigate whether the sensitivity to cisplatin was related to its DNA damage activity, we performed a high-throughput immunofluorescence assay to measure phosphorylation of histone H2AX at Ser139 (γH2AX), an established marker of DNA damage (27, 28). Indeed, *NSD1*-disrupted CAL33 cells had increased γH2AX signal when treated with cisplatin relative to wild-type controls (Materials and Methods, Supplementary Fig. S5A). Because radiation is also standard treatment for patients with HNSCC, we tested whether *NSD1* disruption caused sensitivity to radiation using clonogenic assays on the CAL33 cell line (Materials and Methods). Although the disruption of *NSD1* significantly reduced the formation of colonies (i.e., plating efficiency) relative to wild type (Supplementary Fig. S5B), after normalizing for this effect, we did not observe a significant difference in the radiation dose–response curves for CAL33 ($P = 0.15$, Extra-sum-of-squares F-test, Supplementary Fig. S5C).

Finally, we investigated whether this drug sensitivity was specific to HNSCC, by analyzing a collection of 1,001 cancer cell lines representing a diverse set of tumor types (Supplementary Fig. S6) with full genomic profiles and measured responses to 265 anti-cancer drugs (19). Comparing differential drug sensitivity between cell lines containing at least one *NSD1* allele with a truncating mutation ($n = 17$) and those with wild-type *NSD1* ($n = 774$), we found that drugs targeting DNA replication or genome integrity were more likely to be effective in cell lines with *NSD1* disrupted ($P = 0.003$, Wilcoxon rank sum; Fig. 4D). One of the most effective drugs in this category was cisplatin, with a 24% decrease in IC_{50} relative to wild type ($P = 0.02$, Student *t* test; Fig. 4E). Taken together, these data suggest that *NSD1* loss-of-function

Published OnlineFirst April 10, 2018; DOI: 10.1158/1535-7163.MCT-17-0937

increases sensitivity to DNA damaging chemotherapies, such as cisplatin, and the effect may generalize beyond HNSCC cell lines.

Discussion

Although our study has focused on somatic mutations of a particular gene, *NSD1*, in a particular context, HNSCC, the implications may in fact be broader. *NSD1* is altered in other tumor types, including epigenetic inactivation through promoter hypermethylation in glioma (29) and translocations with a fusion protein in acute myeloid leukemia (*NUP98*/*NSD1*; refs. 30–32). Although *NSD1* has been shown as a biomarker for global epigenetic changes in cancer (33, 34), we have also shown here that *NSD1* is a prognostic biomarker in patients with HPV(−) HNSCC. Beyond *NSD1* itself, the NSD family of HMTs has been linked to various cancers, with *NSD2* mutations seen in breast cancer, lung cancer, and acute myelogenous leukemia (35, 36).

The connection between *NSD1* loss-of-function mutations and CpG hypomethylation is also seen in the germline setting. Patients with Sotos syndrome have inherited loss-of-function mutations in *NSD1* and present clinically with childhood overgrowth, non-progressive developmental delay and a distinctive facial appearance (37). A recent genomic analysis of Sotos syndrome patients found a genome-wide DNA hypomethylation signature that distinguishes them from normal controls (22). The affected genes function in cellular morphogenesis and neuronal differentiation, consistent with the clinical phenotype. Sotos Syndrome follows an autosomal dominant inheritance pattern, consistent with our observation that the *NSD1* truncating mutations found in HNSCC are hemizygous, suggesting that loss of a single copy of *NSD1* is sufficient to cause hypomethylation.

An important question is how *NSD1*, an HMT, can impact methylation of not only histones but also DNA. Indeed, histone methylation and DNA methylation are intertwined in a complex relationship (38), and at least two mechanisms are plausible. First, cells deficient in *NSD1* are unable to mono- and di-methylate H3K36 (39–41). In turn, this defect likely affects the ability of these histones to recruit DNA methyltransferases (34), leading to a global DNA hypomethylation signature. Another connection between HMTs and DNA methylation is that some SET-domain containing HMTs physically recruit DNA methyltransferase leading to CpG methylation (42).

A second question relates to how hypomethylation of DNA is connected to cisplatin sensitivity. Indeed, DNA hypomethylation has been previously implicated as a potential sensitizer for several chemotherapeutic agents, including cisplatin and other platinum-based treatments (23, 24, 43). Treating cisplatin-resistant HNSCC cell lines with decitabine, a cytidine analog that inhibits DNA methylation leading to global DNA hypomethylation, also renders these cells sensitive to cisplatin (25). In diffuse large B-cell lymphoma, treating cells with DNA methyltransferase inhibitors leads to the expression of previously repressed genes and renders these cells sensitive to chemotherapy (26). On the basis some of these observations, combinations of hypomethylating agents and cisplatin have been attempted in head and neck cancer in phase I clinical trials (NCT00901537 and NCT00443261), however both trials were terminated early due to accrual problems. Preliminary results (NCT00901537) show encouraging activity with one partial response, one patient with progression-free survival for 15 months and another with progression free survival for greater than 6 months (44). Given our finding that cells become more sensitive to cisplatin after *NSD1* disruption or pharmacological inhibition of HMTs, perhaps an HMTi could be used along with platinum-based therapy to more effectively treat HPV(−) HNSCC patients. In addition to platinum sensitivity, we also found that disrupting *NSD1* dramatically reduced the clonogenic growth capacity of the CAL33 cell line. This finding may also be related to the survival advantage seen in patients with *NSD1* mutant tumors, and should be studied in a greater number of cell lines across cancer lineages.

Given that *NSD1* mutation is associated with a dramatic increase in the survival of HPV(−) HNSCC patients in multiple cohorts, we propose that patients with loss-of-function *NSD1* mutations should be considered a distinct clinical subclass of HPV(−) HNSCC. In addition to serving as a prognostic biomarker, the *in vitro* cisplatin sensitivity data suggest that *NSD1* mutation is also predictive of response to cisplatin chemotherapy. Although clinical validation of this finding is still needed, our results suggest that cisplatin should be strongly considered for any HNSCC patient with *NSD1* loss-of-function mutation, especially because platinum chemotherapy is already part of the standard of care. Given the clear influence on survival as well as the distinct molecular features of *NSD1* mutant tumors, future prospective clinical trials of HPV(−) HNSCC should include these tumors as a planned subgroup with expected differences in therapeutic response.

Disclosure of Potential Conflicts of Interest

T. Ideker is a consultant/advisory board member for Data4Cure and Ideaya. No potential conflicts of interest were disclosed by the other authors.

Authors' Contributions

Conception and design: N. Bui, J.K. Huang, T. Ideker
Development of methodology: N. Bui, J.K. Huang, A. Bojorquez-Gomez, T. Wang, J.P. Shen, T. Ideker
Acquisition of data (provided animals, acquired and managed patients, provided facilities, etc.): N. Bui, J.K. Huang, A. Bojorquez-Gomez, K. Licon, K.S. Sanchez, S.N. Tang, A.N. Beckett, J.P. Shen, T. Ideker
Analysis and interpretation of data (e.g., statistical analysis, biostatistics, computational analysis): N. Bui, J.K. Huang, T. Wang, W. Zhang, J.P. Shen, J.F. Kreisberg, T. Ideker
Writing, review, and/or revision of the manuscript: N. Bui, J.K. Huang, T. Wang, J.P. Shen, J.F. Kreisberg, T. Ideker
Administrative, technical, or material support (i.e., reporting or organizing data, constructing databases): N. Bui, A. Bojorquez-Gomez, S.N. Tang, T. Wang, J.P. Shen, J.F. Kreisberg, T. Ideker
Study supervision: T. Ideker

Acknowledgments

This work was generously supported by the following grants from the U.S. National Institutes of Health: R01 ES014811, P41 GM103504, and U24 CA184427 (to T. Ideker), U54 CA209891 and P50 GM085764 (to J.F. Kreisberg and T. Ideker), L30 CA171000 (to J.P. Shen), T32 GM008806 (to J.K. Huang), and T32 GM008666 (to T. Wang). J.P. Shen was also supported by a Career Development Grant from the Tower Cancer Research Foundation. The results published here are in part based on data generated by TCGA, established by the National Cancer Institute and the National Human Genome Research Institute, and we are grateful to the specimen donors and relevant research groups associated with this project. We would also like to thank investigators at the University of Chicago for clinical and sequencing data from their head and neck cohort. We would

also like to thank the laboratory of Dr. Mark Tuszynski for use of their imaging equipment for our γH2AX Immunofluorescence assay and the lab of Dr. Silvio Gutkind for helping in the acquisition of the cell lines used.

The costs of publication of this article were defrayed in part by the payment of page charges. This article must therefore be hereby marked *advertisement* in accordance with 18 U.S.C. Section 1734 solely to indicate this fact.

Received September 21, 2017; revised February 6, 2018; accepted April 5, 2018; published first April 10, 2018.

References

1. Jemal A, Bray F, Center MM, Ferlay J, Ward E, Forman D. Global cancer statistics. CA Cancer J Clin 2011;61:69–90.
2. Huang SH, Xu W, Waldron J, Siu L, Shen X, Tong L, et al. Refining American joint committee on cancer/union for international cancer control TNM stage and prognostic groups for human papillomavirus-related oropharyngeal carcinomas. J Clin Oncol 2015;33:836–45.
3. Bhatia A, Burtness B. Human papillomavirus-associated oropharyngeal cancer: defining risk groups and clinical trials. J Clin Oncol 2015;33:3243–50.
4. Hitt R, Grau JJ, López-Pousa A, Berrocal A, García-Girón C, Irigoyen A, et al. A randomized phase III trial comparing induction chemotherapy followed by chemoradiotherapy versus chemoradiotherapy alone as treatment of unresectable head and neck cancer. Ann Oncol 2014;25:216–25.
5. Cohen EE, Karrison TG, Kocherginsky M, Mueller J, Egan R, Huang CH, et al. Phase III randomized trial of induction chemotherapy in patients with N2 or N3 locally advanced head and neck cancer. J Clin Oncol 2014;32:2735–43.
6. Magrini SM, Buglione M, Corvò R, Pirtoli L, Paiar F, Ponticelli P, et al. Cetuximab and radiotherapy versus cisplatin and radiotherapy for locally advanced head and neck cancer: a randomized phase II trial. J Clin Oncol 2016;34:427–35.
7. Buglione M, Maddalo M, Corvò R, Pirtoli L, Paiar F, Lastrucci L, et al. Subgroup analysis according to human papillomavirus status and tumor site of a randomized phase II trial comparing cetuximab and cisplatin combined with radiation therapy for locally advanced head and neck cancer. Int J Radiat Oncol Biol Phys 2017;97:462–72.
8. Cancer Genome Atlas Network. Comprehensive genomic characterization of head and neck squamous cell carcinomas. Nature 2015;517:576–82.
9. Broad Institute TCGA Genome Data Analysis Center. Analysis-ready standardized TCGA data from Broad GDAC Firehose 2016_01_28 run. Broad Institute of MIT and Harvard. Dataset [Internet] 2016.
10. Therneau TM, Grambsch PM. Modeling Survival Data: Extending the Cox Model 2000.
11. Martin D, Abba MC, Molinolo AA, Vitale-Cross L, Wang Z, Zaida M, et al. The head and neck cancer cell oncogenome: a platform for the development of precision molecular therapies. Oncotarget 2014;5:8906–23.
12. Sanjana NE, Shalem O, Zhang F. Improved vectors and genome-wide libraries for CRISPR screening. Nat Methods 2014;11:783–4.
13. Aryee MJ, Jaffe AE, Corrada-Bravo H, Ladd-Acosta C, Feinberg AP, Hansen KD, et al. Minfi: a flexible and comprehensive Bioconductor package for the analysis of Infinium DNA methylation microarrays. Bioinformatics 2014;30:1363–9.
14. Teschendorff AE, Marabita F, Lechner M, Bartlett T, Tegner J, Gomez-Cabrero D, et al. A beta-mixture quantile normalization method for correcting probe design bias in Illumina Infinium 450 k DNA methylation data. Bioinformatics 2013;29:189–96.
15. Varoquaux G, Buitinck L, Louppe G, Grisel O, Pedregosa F, Mueller A. Scikit-learn. GetMobile 2015;19:29–33.
16. Ma A, Yu W, Li F, Bleich RM, Herold JM, Butler KV, et al. Discovery of a selective, substrate-competitive inhibitor of the lysine methyltransferase SETD8. J Med Chem 2014;57:6822–33.
17. Franken NAP, Rodermond HM, Stap J, Haveman J, van Bree C. Clonogenic assay of cells in vitro. Nat Protoc 2006;1:2315–9.
18. Barendsen GW.Parameters of linear-quadratic radiation dose-effect relationships: dependence on LET and mechanisms of reproductive cell death. Int J Radiat Biol 1997;71:649–55.
19. Iorio F, Knijnenburg TA, Vis DJ, Bignell GR, Menden MP, Schubert M, et al. A landscape of pharmacogenomic interactions in cancer. Cell 2016;166:740–54.
20. Lawrence MS, Stojanov P, Polak P, Kryukov GV, Cibulskis K, Sivachenko A, et al. Mutational heterogeneity in cancer and the search for new cancer-associated genes. Nature 2013;499:214–8.
21. Seiwert TY, Zuo Z, Keck MK, Khattri A, Pedamallu CS, Stricker T, et al. Integrative and comparative genomic analysis of HPV-positive and HPV-negative head and neck squamous cell carcinomas. Clin Cancer Res 2015;21:632–41.
22. Choufani S, Cytrynbaum C, Chung BHY, Turinsky AL, Grafodatskaya D, Chen YA, et al. NSD1 mutations generate a genome-wide DNA methylation signature. Nat Commun 2015;6:10207.
23. Fu S, Hu W, Iyer R, Kavanagh JJ, Coleman RL, Levenback CF, et al. Phase 1b-2a study to reverse platinum resistance through use of a hypomethylating agent, azacitidine, in patients with platinum-resistant or platinum-refractory epithelial ovarian cancer. Cancer 2011;117:1661–9.
24. Asadollahi R, Hyde CAC, Zhong XY. Epigenetics of ovarian cancer: from the lab to the clinic. Gynecol Oncol 2010;118:81–7.
25. Viet CT, Dang D, Achdjian S, Ye Y, Katz SG, Schmidt BL. Decitabine rescues cisplatin resistance in head and neck squamous cell carcinoma. PLoS ONE 2014;9:e112880.
26. Clozel T, Yang S, Elstrom RL, Tam W, Martin P, Kormaksson M, et al. Mechanism-based epigenetic chemosensitization therapy of diffuse large B-cell lymphoma. Cancer Discov 2013;3:1002–19.
27. Sharma A, Singh K, Almasan A. Histone H2AX phosphorylation: a marker for DNA damage. Methods Mol Biol 2012;920:613–26.
28. Paull TT, Rogakou EP, Yamazaki V, Kirchgessner CU, Gellert M, Bonner WM. A critical role for histone H2AX in recruitment of repair factors to nuclear foci after DNA damage. Curr Biol 2000;10:886–95.
29. Berdasco M, Ropero S, Setien F, Fraga MF, Lapunzina P, Losson R, et al. Epigenetic inactivation of the Sotos overgrowth syndrome gene histone methyltransferase NSD1 in human neuroblastoma and glioma. Proc Natl Acad Sci U S A 2009;106:21830–5.
30. Xu H, Valerio DG, Eisold ME, Sinha A, Koche RP, Hu W, et al. NUP98 fusion proteins interact with the NSL and MLL1 complexes to drive leukemogenesis. Cancer Cell 2016;30:863–78.
31. Struski S, Lagarde S, Bories P, Puiseux C, Prade N, Cuccuini W, et al. NUP98 is rearranged in 3.8% of pediatric AML forming a clinical and molecular homogenous group with a poor prognosis. Leukemia 2017;31:565–72.
32. Hollink IH, van den Heuvel-Eibrink MM, Arentsen-Peters ST, Pratcorona M, Abbas S, Kuipers JE, et al. NUP98/NSD1 characterizes a novel poor prognostic group in acute myeloid leukemia with a distinct HOX gene expression pattern. Blood 2011;118:3645–56.
33. Lee ST, Wiemels JL. Genome-wide CpG island methylation and intergenic demethylation propensities vary among different tumor sites. Nucleic Acids Res 2016;44:1105–17.
34. Papillon-Cavanagh S, Lu C, Gayden T, Mikael LG, Bechet D, Karamboulas C, et al. Impaired H3K36 methylation defines a subset of head and neck squamous cell carcinomas. Nat Genet 2017;49:180–5.
35. Morishita M, di Luccio E. Cancers and the NSD family of histone lysine methyltransferases. Biochim Biophys Acta 2011;1816:158–63.
36. He C, Li F, Zhang J, Wu J, Shi Y. The methyltransferase NSD3 has chromatin-binding motifs, PHD5-C5HCH, that are distinct from other NSD (nuclear receptor SET domain) family members in their histone H3 recognition. J Biol Chem 2013;288:4692–703.
37. McClelland J, Burgess B, Crock P, Goel H. Sotos syndrome: an unusual presentation with intrauterine growth restriction, generalized lymphedema, and intention tremor. Am J Med Genet A 2016;170A:1064–9.
38. Tamaru H, Selker EU. A histone H3 methyltransferase controls DNA methylation in Neurospora crassa. Nature 2001;414:277–83.
39. Qiao Q, Li Y, Chen Z, Wang M, Reinberg D, Xu RM. The structure of NSD1 reveals an autoregulatory mechanism underlying histone H3K36 methylation. J Biol Chem 2011;286:8361–8.

Published OnlineFirst April 10, 2018; DOI: 10.1158/1535-7163.MCT-17-0937

40. Suzuki S, Murakami Y, Takahata S. H3K36 methylation state and associated silencing mechanisms. Transcription 2016;8:26–31.
41. Mutations in histone H3K36 prevent methylation and drive sarcomagenesis. Cancer Discov 2016;6:689.
42. Cedar H, Bergman Y. Linking DNA methylation and histone modification: patterns and paradigms. Nat Rev Genet 2009;10:295–304.
43. Li M, Balch C, Montgomery JS, Jeong M, Chung JH, Yan P, et al. Integrated analysis of DNA methylation and gene expression reveals specific signaling pathways associated with platinum resistance in ovarian cancer. BMC Med Genomics 2009;2:34.
44. Liao YM, Mirshahidi H, Zhang K, Mirshahidi S, Williamson S, Hsueh CT. Abstract 2663: phase I study of azacitidine and cisplatin in patients with advanced head and neck or non-small cell lung cancer. Cancer Res 2012; 72:2663.
45. Mermel CH, Schumacher SE, Hill B, Meyerson ML, Beroukhim R, Getz G. GISTIC2.0 facilitates sensitive and confident localization of the targets of focal somatic copy-number alteration in human cancers. Genome Biol 2011;12:R41.
46. Gao J, Aksoy BA, Dogrusoz U, Dresdner G, Gross B, Sumer SO, et al. Integrative analysis of complex cancer genomics and clinical profiles using the cBioPortal. Sci Signal 2013;6:11.
47. Cerami E, Gao J, Dogrusoz U, Gross BE, Sumer SO, Aksoy BA, et al. The cBio cancer genomics portal: an open platform for exploring multidimensional cancer genomics data. Cancer Discov 2012;2:401–4.

Published OnlineFirst April 10, 2018; DOI: 10.1158/1535-7163.MCT-17-0937

Molecular Cancer Therapeutics

Disruption of *NSD1* in Head and Neck Cancer Promotes Favorable Chemotherapeutic Responses Linked to Hypomethylation

Nam Bui, Justin K. Huang, Ana Bojorquez-Gomez, et al.

Mol Cancer Ther 2018;17:1585-1594. Published OnlineFirst April 10, 2018.